



UNITED NATIONS EDUCATIONAL, SCIENTIFIC AND CULTURAL ORGANIZATION  
INTERNATIONAL ATOMIC ENERGY AGENCY  
INTERNATIONAL CENTRE FOR THEORETICAL PHYSICS  
I.C.T.P., P.O. BOX 586, 34100 TRIESTE, ITALY, CABLE: CENTRATOM TRIESTE



H4.SMR/984-17

## Winter College on Quantum Optics: Novel Radiation Sources

3-21 March 1997

*Beyond lasing without inversion*

*PART II*

M.O. Scully

Department of Physics, Texas A&M University, College Station, TX, USA

# Counter-counterintuitive Quantum Coherence Effects \*

Marlan O. Scully<sup>1,2</sup>, Chris J. Bednar<sup>1</sup>, Yuri Rostovtsev<sup>1</sup>, and Shi-Yao Zhu<sup>3</sup>

<sup>1</sup>*Department of Physics, Texas A&M University,  
College Station, TX 77843-4242*

<sup>2</sup>*Max-Planck-Institut für Quantenoptik,  
Hans-Kopfermann-Str. 1,  
D-85748, Garching, Germany*

<sup>3</sup>*Department of Physics,  
Hong Kong Baptist University,  
Hong Kong  
(March 7, 1997)*

The study of an ensemble of phase-coherent atoms has recently lead to interesting theoretical innovations and experimental demonstrations of counterintuitive effects such as electromagnetically induced transparency (EIT), lasing without inversion (LWI), enhancement of index of refraction, and ultra-large nonlinear susceptibility.

In the present notes, we report a couple of new effects along these lines. In fact, it would be fair to call them surprises even in the repertoire of "counterintuitive effects", i.e., "counter-counterintuitive effects". Specifically, we will show that the LWI concept, which is based on quantum coherence, has a surprising counterpart in the classical physics of free electron laser operation.

In other current work, we find that it is possible to "lock" atoms in an excited state via atomic coherence. It is, by now, not surprising that such a phase-coherent ensemble can show holes or dark lines in the emission spectrum. It is surprising that we can lock atoms in an excited (normally decaying) state via atomic coherence and interference. Such a phase-coherent collection of atoms, i.e. "phaseonium", is indeed a novel new state of matter.

## I. THE FREE ELECTRON PHASER (FEP): A PHASE-SENSITIVE OPTICAL KLYSTRON

In a free-electron laser (FEL) [1], electrons are accelerated by a "pondermotive potential" formed by the combined field of the wiggler and the laser, and this produces coherent stimulated radiation. Under the influence of the pondermotive potential, a grating in the spatial density of electrons ("bunching") on the scale of the laser wavelength is produced. As a result net emission may be enhanced. If the current of electrons in the beam is high enough, or, equivalently, if the wiggler is long enough, bunching is significant and the gain is greatly increased; this leads to the "large gain" regime [2].

A main limitation on gain is set by the spread in the longitudinal momentum of electrons in the beam. For this reason, much effort has been devoted to producing highly monoenergetic electron beams [3].

Recently new approaches to the increase of gain in atomic lasers based on coherence and interference have lead to lasing without inversion [4]. This concept has interesting implications for the FEL (a purely classical device!) as well. It is conceptually implemented by an appropriate phasing of the electrons in the drift region between two wigglers via a static magnetic field.

Introduce the detuning  $\Omega$  as the difference of electron momentum from resonant momentum

$$\Omega = \frac{k_L + k_W}{m\gamma^3}(p - p_r),$$

where the resonant momentum is connected with phase velocity of the pondermotive potential

$$v_r = \frac{\omega_L - \omega_W}{k_L + k_W},$$

as  $p_r = m\gamma_r v_r$  and the resonant Lorentz factor is

$$\gamma_r = \frac{1}{\sqrt{1 - \frac{v_r^2}{c^2}}},$$

---

\*Based on a lecture given by Marlan Scully to the Royal Society, London, January 1997

where  $k_W, \omega_W$  are wave vector and frequency of wiggler field, and  $k_L, \omega_L$  are wave vector and effective frequency of laser field. The electron motion inside the wiggler depends on the phase of laser field at the moment the electron enters the ponderomotive potential. Due to motion in the drift region the phase of the electron relative to the laser field changes: slow electrons (path 2) travel further due to the static  $B$ -field than do the fast ones (path 1). If  $\Omega_0$  is the detuning at the entrance of the first wiggler, we can express the phase-shift leading to cancellation of absorption for the electrons having  $\Omega_0 < 0$  and to positive gain for  $\Omega_0 > 0$  [5] as:

$$\Delta\phi = \begin{cases} \pi - \Omega L_W, & \Omega_0 < 0 \\ -\Omega L_W, & \Omega_0 > 0, \end{cases} \quad (1)$$

where  $L_W$  is the dimensionless wiggler length.

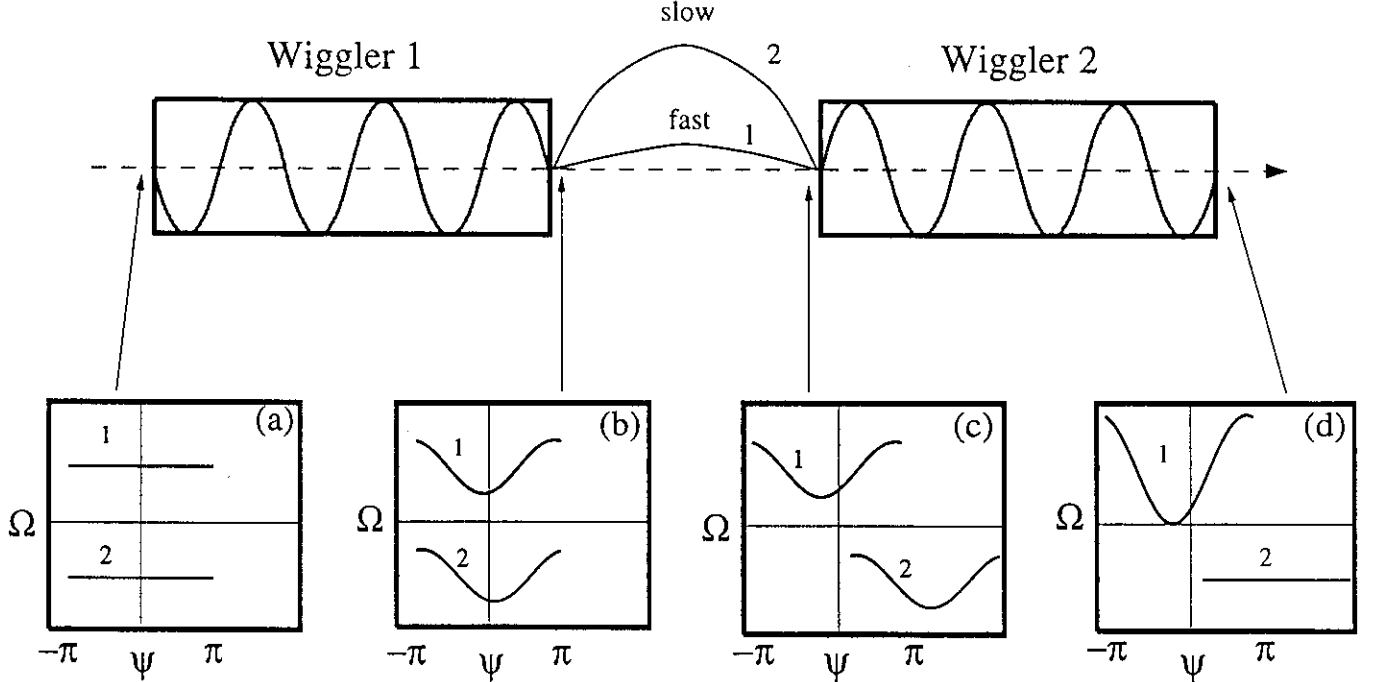


FIG. 1. Snapshots of phase-space motion for fast (1) and slow (2) electrons.  $\psi \equiv (k_L + k_W)z - (\omega_L - \omega_W)t + \phi$  is the total phase of an electron relative to the ponderomotive potential. (a) initial distribution of electrons before entering in wigglers; (b) after the first wiggler; (c) after the drift region: travelling in the static magnetic field the electrons pass along different paths depending on their detunings; (d) after the second wiggler, electrons with negative detuning return to their original energy states, and so do not absorb energy from the field. Fast electrons, however, do lose energy to the field; therefore, there is only gain.

Phase-space motion (see in Fig. 1) provides a way to achieve this cancellation. At the entrance of the first wiggler (Fig. 1a) we have electrons with the same detuning but different initial phases. The slow electrons acquire an extra  $\pi$  phase shift added by the drift region, which reverses the motion of the electron in the second wiggler. After the second wiggler (in Fig. 1d) there is no spread of electrons with negative detuning and consequently no absorption, but there is gain for electrons having positive detuning, i.e., we have LWI.

Let us remark that the realization of the phase-shift (1) is not trivial, because of its dependence on the entrance detuning, as it has been shown in [6]. This can be achieved by oblique propagation of laser field to the wiggler axis (2-dimensional motion allows to determine the initial detuning). This is referred to as a 2-dimensional phased klystron, or free-electron phaser (FEP).

## II. QUENCHING OF SPONTANEOUS EMISSION VIA ATOMIC PHASE COHERENCE

### A. Driven 4-level atom

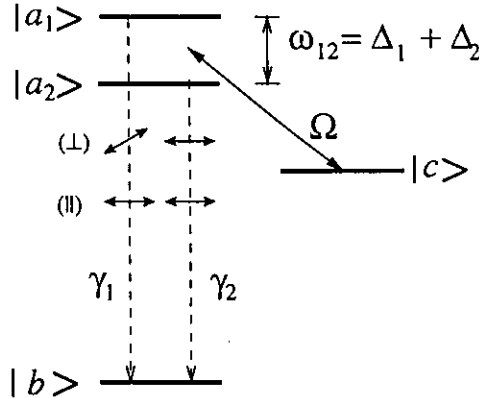


FIG. 2. Two upper levels  $|a_1\rangle$  and  $|a_2\rangle$  are coupled to the ground state  $|b\rangle$  by vacuum modes and to an auxiliary level  $|c\rangle$  by a coherent drive. The dipole elements for the  $a \rightarrow c$  transitions may be either perpendicular ( $\perp$ ) or parallel ( $\parallel$ ).  $\Omega$  is the drive field,  $\omega_{12}$  is the frequency difference between  $|a_1\rangle$  and  $|a_2\rangle$ , and  $\Delta_1$  and  $\Delta_2$  are the detunings of the drive from  $|a_1\rangle$  and  $|a_2\rangle$ , respectively.

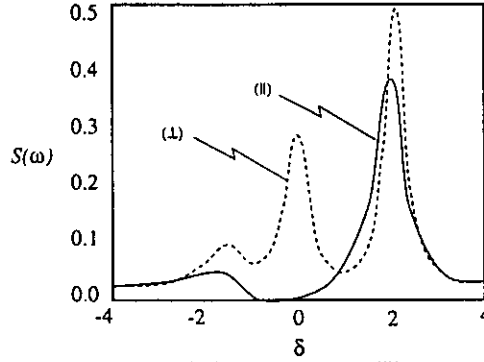


FIG. 3. Spontaneous emission spectra for orthogonal ( $\perp$ ) and parallel ( $\parallel$ ) transition dipole matrix elements. The atom is initially in state  $|a_1\rangle$  (Fig. 2).

As a first example of a phase-coherent medium showing atoms “locked” in an excited configuration, consider a four-level atom that consists of two upper levels  $|a_1\rangle$  and  $|a_2\rangle$ , and an intermediate level  $|c\rangle$  [8]. The two upper levels are coupled by the vacuum to the lower level  $|b\rangle$ . If the dipole elements for the two transitions are parallel, they are coupled by the same vacuum modes; see Fig. 2.

The spontaneous emission spectra for orthogonal ( $\perp$ ) and parallel ( $\parallel$ ) dipole elements (Fig. 2) are quite different due to quantum interference. It is well known that the spontaneous emission spectrum for the orthogonal ( $\perp$ ) case is a three-peak distribution. For parallel ( $\parallel$ ), however, we have interference, which can lead to the elimination of one of the three peaks. In Fig. 3, we plot spectra for both cases with the atom initially in  $|a_1\rangle$ . We see the disappearance of the central peak as a result of interference<sup>1</sup>. The elimination of the central peak indicates the cancellation of the spontaneous emission into those modes with frequencies near the central peak (in the neighborhood of the driving field frequency) and is the result of destructive interference.

The area under the spectral curve is proportional to the energy emitted by the atom into the vacuum modes. For orthogonal polarizations, the area is always equal to unity (energy conservation), that is to say that the atom will

<sup>1</sup>It can be proven analytically that the central peak is eliminated if  $\Delta_2 = -\chi^2 \Delta_1$ , where  $\chi = |\Omega_2/\Omega_1| = g^{(2)}/g^{(1)}$  is the ratio of dipole moments between the upper two levels and level  $|c\rangle$ , which is also equal to the ratio of the dipole moments between the two upper levels and level  $|b\rangle$ ; see Zhu and Scully [8].

finish in the lower level  $|b\rangle$ . For parallel polarization, we find that the area may be less than unity, and we may conclude on this basis that spontaneous emission in this case is canceled by quantum interference, i.e., the atom can live forever in the excited state.

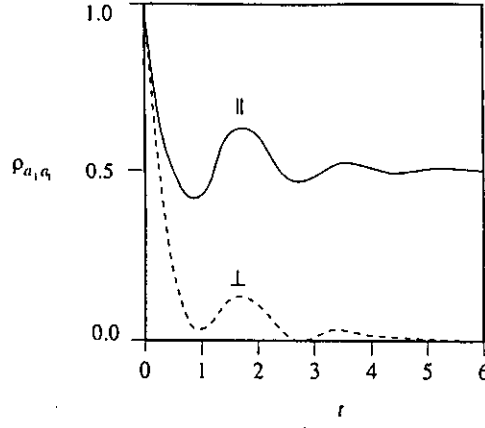


FIG. 4. Time evolution of population in  $|a_1\rangle$  (see Fig. 3) for orthogonal ( $\perp$ ) and parallel ( $\parallel$ ) dipole moments.

In Fig. 4, we plot the evolution of the population in level  $|a_1\rangle$  for both polarizations. It is clear that this population goes to zero for orthogonal, and  $\approx 50\%$  for parallel polarizations. Cancellation of spontaneous emission in the steady state is another example of quantum interference.

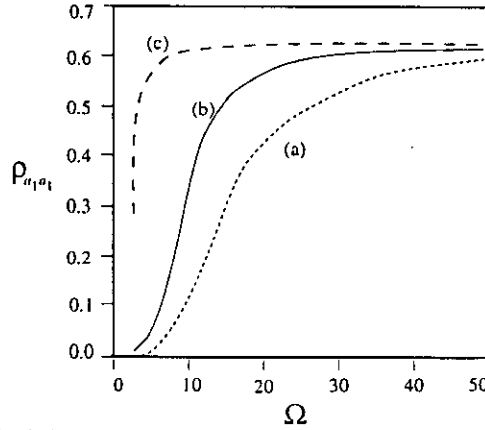


FIG. 5. Trapped population in level  $|a_1\rangle$  (see Fig. 3) versus drive Rabi frequency  $\Omega$  for various values of  $\omega_{12}$ : (a)  $40\gamma_1$ , (b)  $20\gamma_1$ , and (c)  $4\gamma_1$ .

In Fig. 5, we plot the population in level  $|a_1\rangle$  versus the Rabi frequency for three cases with  $\chi = 2$  (see footnote 1 on page 3). It can be seen that 30% of the population will be trapped in level  $|a_1\rangle$  if the Rabi frequency is  $10\gamma_1$  for a large separation ( $\omega_{12} = 40\gamma_1$ ). In order to trap more population, we need a higher Rabi frequency.

Spectral truncation and cancellation of spontaneous emission can be understood in a dressed-state picture. On diagonalizing the Hamiltonian for  $|a_1\rangle$  and  $|a_2\rangle$ ,  $|b\rangle$  and the driving field, we get three dressed states. The decay from  $|a_1\rangle$  and  $|a_2\rangle$  to  $|b\rangle$  becomes the decay from the dressed states to  $|b\rangle$ . The interference in the parallel ( $\parallel$ ) case results in a zero decay rate. The population in one of the dressed states will not decay to lower level  $|b\rangle$ , and consequently we have central peak elimination and spontaneous emission cancellation in steady state.

### B. Three-level atom (no drive) in photonic band-gap material

Now, let us consider the case of a three-level atom (Fig. 6) embedded in a “photonic crystal” [9,10]. Assume the edge of the photonic band gap is located between levels  $|a_1\rangle$  and  $|a_2\rangle$ . The dispersion relation near the band edge can be approximately written as  $\omega = \omega_c + A(k - k_0)^2$ . Therefore, level  $|a_2\rangle$  is within the band gap, while level  $|a_1\rangle$  is in the band. In the band gap, the density of states is zero. There is a singularity in the density of states at  $\omega = 0$ . For  $\omega > \omega_c$ , the density of states decreases. The spontaneous emission of an atom embedded in a photonic band gap

crystal is quite different from the spontaneous emission in a vacuum. Population can be trapped in the two upper levels due to (a) the photonic band gap, and (b) the interference between the two transitions. With interference, we can trap more population in the two upper levels if we prepare the atom in a special initial state. One might think that the largest amount of population would be trapped in the upper levels if the atom were initially prepared in the level within the gap (level  $|a_2\rangle$ ) because of the low density of states. In fact, this is not the case.

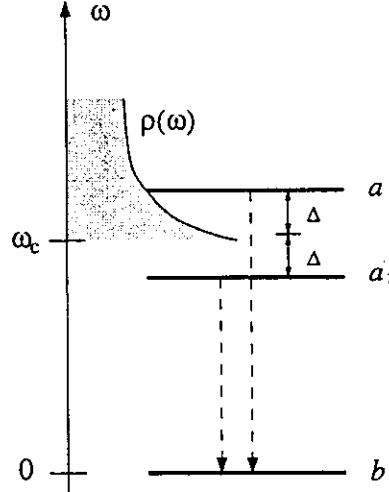


FIG. 6. The scheme: a three-level atom in a photonic band-gap structure (represented by the gray-shaded curve). The upper levels  $|a_1\rangle$  and  $|a_2\rangle$  are placed symmetrically from the band gap edge.

The amount of population trapped in the upper levels depends on the initial condition. The population in the upper level within the band gap ( $|a_2\rangle$ ) can be transferred to the upper level in the transmitting band ( $|a_1\rangle$ ) via emission and reabsorption of a photon. The final state contains an upper level part (trapped excited state population) and a lower level part with one photon in the localized mode. The phase difference between the two upper levels in the final state turns out to be zero. The dependence of the ratio of the populations in the upper two levels,  $A^{(1)}(\infty)/A^{(2)}(\infty)$  on the initial state is weak. This ratio, as well as the portion in the lower level, depends on  $\Delta/\gamma$ .

Since the true trapped final state is a dressed state with a lower-level component, no superposition of the upper levels can evade decay completely. This is in contrast with the dark state of a driven four-level system. However, if the atom is prepared in a state which is a normalized version of this final state projected onto the manifold of the two upper levels

$$|\psi(0)\rangle = \frac{A^{(1)}(\infty)|a_1\rangle + A^{(2)}(\infty)|a_2\rangle}{\sqrt{|A^{(1)}|^2 + |A^{(2)}|^2}}, \quad (2)$$

we can minimize the energy emitted and have more population trapped in the upper levels, even more than the case with the atom in the level in the gap ( $|a_2\rangle$ ), due to quantum interference.

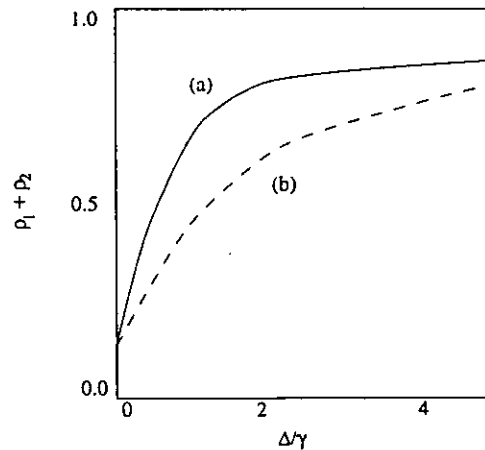


FIG. 7. Sum of populations in states  $|a_1\rangle$  and  $|a_2\rangle$  as a function of  $\Delta$ . (a) initial condition given by Eq. (2), (b)  $|\psi(0)\rangle = |a_2\rangle$ .

## ACKNOWLEDGMENTS

The authors gratefully acknowledge support from the Office of Naval Research, the Welch Foundation and the Texas Advanced Research and Technology Program. YVR wishes to thank the North Atlantic Treaty Organization for support under a grant awarded in 1996.

## REFERENCES

---

- [1] C. A. Brau, *Free-Electron Lasers* (Academic, Boston, 1990);  
G. Dattoli, A. Renieri, and A. Torre, *Lectures on the Free Electron Laser Theory and Related Topics* (World Scientific, London, 1993).
- [2] R. Bonifacio, C. Pellegrini, L.M. Narducci, *Opt. Commun.* **50**, 373 (1984);  
J.B. Murphy, C. Pellegrini, R. Bonifacio, *Opt. Commun.* **53**, 197 (1985)
- [3] A.M. Sessler, D.H. Whitum, Li-Hua Yu, *Phys. Rev. Lett* **68**, p. 309 (1992);  
T. Yamazaki, K. Yamada, S. Sugiyama, et al. *Nucl. Instrum. Methods A*, **331**, 27 (1993);  
M.E. Couprie, T. Hara, D. Gontier, et al., *Phys. Rev. E* **53**, p. 1871 (1996).
- [4] O.A. Kocharovskaya, Ya.I. Khanin, *Pis'ma Zh. Eksp. Teor. Fiz.* **48**, 581 (1988) [JETP Lett. **48**, 630 (1988)];  
S.E. Harris, *Phys. Rev. Lett.* **62**, 1033, 1989;  
M.O. Scully, S.-Y. Zhu, A. Gavrielides, *Phys. Rev. Lett.* **62**, 2813 (1989);  
K.J. Boller, A. Imamoglu, S.E. Harris, *Phys. Rev. Lett.* **66**, 2593, 1991;  
K. Hakuta, L. Marmet, B. Stoicheff, *Phys. Rev. Lett.* **66**, 596 (1991);  
Kocharovskaya O., 1995, *Laser Physics* **5**, 284;  
Zibrov, A.S., et al., 1995, *Phys. Rev. Lett.* **75**, 1499;  
G.G. Padmabandu et al., *Phys. Rev. Lett.* **76**, 2053 (1996).
- [5] D.E. Nikonov, B. Sherman, G. Kurizki, and M.O. Scully, *Opt. Commun.* **123**, 363 (1996);  
D.E. Nikonov, G. Kurizki, and M.O. Scully, *Phys. Rev. E* **45**, 6780 (1996).
- [6] D. Nikonov, Yu. Rostovtsev, and M.O. Scully (to be published).
- [7] J.M.J. Madey, *J. Appl. Phys.* **42**, 1906 (1971).
- [8] S. Y. Zhu and M. O. Scully, *Phys. Rev. Lett.* **76**, 388 (1996);  
H. R. Xia, C. Y. Ye, and S. Y. Zhu, *Phys. Rev. Lett.* **76**, 1032 (1996).
- [9] S. John and J. Wang, *Phys. Rev. Lett.* **64**, 2418 (1990); S. John and J. wang, *Phys. Rev. B* **43**, 12772 (1991)
- [10] S. John and T. Quang, *Phys. Rev. A* **50**, 1764 (1994)





# Experimental Demonstration of Enhanced Index of Refraction via Quantum Coherence in Rb

A. S. Zibrov,<sup>1,2,4,5</sup> M. D. Lukin,<sup>1,2,3</sup> L. Hollberg,<sup>4</sup> D. E. Nikonov,<sup>1,2,3</sup> M. O. Scully,<sup>1,2,3</sup> H. G. Robinson,<sup>4</sup>  
and V. L. Velichansky<sup>5</sup>

<sup>1</sup>Department of Physics, Texas A&M University, College Station, Texas 77843

<sup>2</sup>Texas Laser Laboratory, HARC, The Woodlands, Texas 77381

<sup>3</sup>Max-Planck-Institut für Quantenoptik, D-85748 Garching, Germany

<sup>4</sup>National Institute of Standards and Technology, Boulder, Colorado 80303

<sup>5</sup>Lebedev Institute of Physics, 117924 Moscow, Russia

(Received 11 December 1995)

We present a proof-of-principle experiment demonstrating a resonant enhancement of the index of refraction accompanied by vanishing absorption in a cell containing a coherently prepared Rb vapor. The results are in good agreement with detailed theoretical predictions. [S0031-9007(96)00142-1]

PACS numbers: 42.50.Ar, 42.55.-f

In the present Letter we report the first demonstration of a resonant enhancement of the index of refraction without absorption [1]. Surprising and counterintuitive effects involving quantum coherence and interference have recently become laboratory realities. For example, phenomena such as electromagnetically induced transparency (EIT) [2] and lasing without population inversion (LWI) [3], predicted theoretically at the end of the 1980s have now been demonstrated experimentally [4–7]. In both of the above effects quantum coherence dramatically modifies the *absorptive* properties of the medium. The unusual behavior of the *dispersive* part of the susceptibility of coherently prepared medium is no less intriguing. For example, it was shown theoretically that it is possible to have a completely transparent medium with large dispersion (i.e., rapid variation of index of refraction with frequency) or with large index of refraction [1]. Both of these effects can be achieved using atomic phase coherence in a resonant medium, which is normally optically thick. Coherence effects, however, allow us to prepare an optical medium such that the medium has vanishing absorption, while the dispersive part of the susceptibility is enhanced.

The interest in these phenomena is due, on one hand, to the fundamental nature of coherence effects and, on the other hand, to possible applications. For example, the dispersive properties of coherently prepared media have been studied with an eye toward generation of pulses with very slow group velocity [8], effective control of nonlinearities [9], high precision magnetometry [10], and laser acceleration of particles [1].

Several recent experiments [11] have demonstrated the large dispersion of the index of refraction accompanying EIT. Index enhancement, however, allows not only for large dispersion, but also for a large refractive index itself, while maintaining a transparent medium.

The conceptual foundation of the present experiment can be understood by considering the simple  $\Lambda$  atomic configuration of Fig. 1. The coherent strong driving field with Rabi frequency ( $\Omega$ ) and weak coherent probe ( $\Omega_p$ )

allow us to prepare the atom in a coherent superposition of states  $b$  and  $c$  [12]. When the detunings of these two fields from their respective atomic resonances are equal, EIT is obtained. The incoherent pumping (represented by the rate  $r$ ) alters this coherent superposition by pumping some of the population into other states. Depending upon the actual parameters of the system this may result in gain, loss, or complete transparency for the probe field.

The linear gain (absorption) coefficient ( $G$ ) is proportional to the imaginary part of complex susceptibility ( $\chi''$ ). In the case when the driving field is in exact resonance with transition  $a \rightarrow c$  it is given for this particular three-level configuration by [13]

$$G = \kappa \frac{\gamma_{bc} A (\gamma_{cb} \gamma_{ab} + |\Omega|^2 - \Delta^2) + \Delta^2 B (\gamma_{ab} + \gamma_{bc})}{(\gamma_{bc} \gamma_{ab} + |\Omega|^2 - \Delta^2)^2 + \Delta^2 (\gamma_{ab} + \gamma_{bc})^2}, \quad (1)$$

where  $\kappa = 3\lambda^2 N \gamma_a' L / 4\pi$ , and  $A$  and  $B$  are given by

$$A = [1 + (\gamma_a' + \gamma_a'') / 2\gamma_{bc}] \rho_{aa} - \rho_{bb}, \quad (2)$$

$$B = \rho_{aa} - \rho_{bb}. \quad (3)$$

Here  $\rho_{ii}$  is the population of level  $i$  calculated to the zeroth order in the probe field,  $\gamma_{ij}$  is the relaxation rate of the density matrix element  $\rho_{ij}$ ,  $N$  is the density of atoms,  $L$  is the length of the cell,  $\lambda$  is the wavelength,

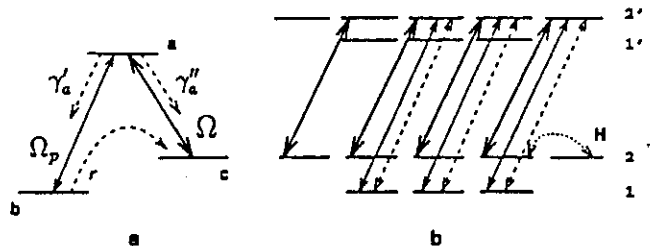


FIG. 1. (a) Simplified three-level model for index enhancement. (b) The actual level scheme of  $D_1$  absorption line in Rb<sup>87</sup> and the optical fields used in the present experiment. Energy separation between manifolds 1 and 2 is equivalent to 6.8 GHz.

$\Delta$  is the detuning of the probe laser, and atomic decays ( $\gamma'_a, \gamma''_a$ ) are indicated in Fig. 1(a). For the case  $\Delta = 0$  we see that, in the presence of the coherent driving field, the gain (which is in that case proportional to  $A$ ) can be positive even if most population remains in the ground state  $b$ , i.e., even if  $B < 0$ . That is, a weak probe field undergoes amplification without the need of population inversion [7,14]. If the probe field is detuned from atomic resonance, the gain coefficient decreases rapidly, and vanishes when

$$\Delta = \Delta_0 = \pm \sqrt{\frac{A\gamma_{bc}(\Omega^2 + \gamma_{ab}\gamma_{bc})}{A\gamma_{bc} - B(\gamma_{ab} + \gamma_{bc})}}. \quad (4)$$

Let us turn now to the real part of the complex susceptibility ( $\chi'$ ), i.e., to the resonant index of refraction. It results, in particular, in the phase shift ( $\phi$ ) for the probe light transmitted through the resonant vapor, which is proportional to  $\chi'$ :

$$\phi = -\frac{\kappa}{2} \Delta \frac{B(\gamma_{cb}\gamma_{ab} + |\Omega|^2 - \Delta^2) - A(\gamma_{ab} + \gamma_{bc})\gamma_{bc}}{(\gamma_{cb}\gamma_{ab} + |\Omega|^2 - \Delta^2)^2 + \Delta^2(\gamma_{ab} + \gamma_{bc})^2}. \quad (5)$$

The phase shift is equal to zero when the probe field is tuned precisely to the resonance with the  $a \rightarrow b$  transition, but for nonzero probe field detuning it can become quite large. To be more specific, we consider the system with decay rates and pumping as indicated in Fig. 1(a) [13]. In this case and if we take  $r \sim \gamma'_a \sim \gamma''_a, \Omega \gg \sqrt{\gamma_{ab}r}$ , the gain coefficient vanishes at  $\Delta_0 \sim \pm \sqrt{|\Omega_d|^2 + \gamma_{ab}\gamma_{bc}}$ . At this point the phase shift is on the order of

$$\phi(\Delta_0) \sim (\kappa/12)/\Delta_0. \quad (6)$$

It follows, therefore, that a medium can become transparent at the point where the resonant index of refraction has a large value.

A  $\Lambda$ -type atomic configuration can be realized within the  $D_1$  absorption line of Rb as shown in Fig. 1(b). Here right circularly polarized coherent driving and probe fields are tuned close to the  $2 \rightarrow 2'$  and  $1 \rightarrow 2'$  transitions, respectively [15]. The incoherent pumping out of the states 1 is accomplished by a broadband right circularly polarized field which couples the transition  $1 \rightarrow 2'$ . All of the fields are copropagating, which allows for the reduction of Doppler broadening.

We note here that optical properties of the real atomic systems are, in general, different from those of simplified 3- or 4-level models due to the presence of many hyperfine and Zeeman sublevels. In particular, optical pumping can play an important role. Indeed, in the case when both driving and pumping fields are present, atoms can be optically pumped into the state  $F = 2, M_F = +2$  [Fig. 1(b)]. To avoid the trapping of the population in this state a weak magnetic field ( $\sim 2 \times 10^{-4}$  T) is used, which mixes the populations via Larmor precession.

In order to account for realistic experimental conditions we developed a numerical model, wherein the field polar-

izations, the presence of hyperfine and Zeeman sublevels and Doppler broadening are taken into account. This is done by numerically solving the density matrix equations for the 16-level system of Fig. 1(b) and averaging over a Maxwell velocity distribution. The numerical analysis showed that for parameters typical of our experiment the effect of index enhancement depends upon the tuning of the drive laser within the Doppler absorption profile. This is the case when the intensity of a driving field is relatively low and the ground state relaxation rate is sufficiently high (determined in our case by the incoherent pump rate). Under these conditions we found the index enhancement is larger if the driving field is detuned to either side of the center of the Doppler profile by roughly a third of the Doppler width.

The results of the calculations are presented in Fig. 2. They clearly show that there is a region (indicated by  $I$ ) where absorption is canceled and, at the same time, the real part of susceptibility (i.e., the phase shift) increases due to the presence of the drive and pump fields.

In the experiment we used a 4 cm long cell containing natural Rb. Drive and probe lasers were extended cavity diode lasers at 794 nm with linewidths of about 100 kHz. The powers of these beams in the region of the cell were on the order of 10 mW and 5  $\mu$ W, respectively, and the corresponding spot sizes in the same region were 2 mm and 100  $\mu$ m. The angle between two beams did not exceed  $5 \times 10^{-3}$  rad. The pump laser was a solitary laser diode (794 nm) with output power  $\approx 5$  mW. Its linewidth was additionally broadened to about 150 MHz

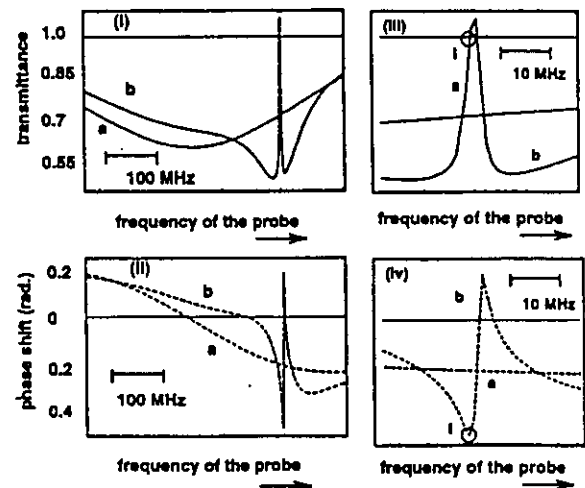


FIG. 2. Calculated absorption coefficient (i,iii) and phase shift (ii,iv) of the probe field in the Rb vapor. In all figures curve (a) corresponds to the case without driving and pumping fields, curve (b) corresponds to the case when these two fields are present. Parameters for numerical modeling are  $\Omega = 16$  MHz, Doppler width is 500 MHz, incoherent pump corresponds to  $r = 0.5$  MHz, and magnetic field  $H_z = 2 \times 10^{-4}$  T. Natural linewidth of the Rb  $D_1$  absorption line is 5.4 MHz.

by modulating the diode's input current with noise. The size of the pump beam was on the order of  $3 \times 5$  mm.

The resonant index of refraction was determined via phase-shift measurements using a Mach-Zehnder interferometer (see Fig. 3). When the interferometer arms are of nearly equal length the difference current of photodetectors PD1 and PD2 is proportional to

$$S_{\text{signal}} \sim I_0 \exp(G/2) \sin(\phi + \phi_0), \quad (7)$$

where  $I_0$  is the intensity of the probe field and  $\phi_0$  is a constant phase shift determined by a balance of the interferometer arms. A piezoelectric transducer is used to vary  $\phi_0$  and thus obtain the scaling of the signal.

The first experiments were carried out with the low Rb density, such that maximum probe absorption was on the order of 40%. Under these conditions the signal given by Eq. (7) is the phase shift of the probe field in the Rb cell, provided that the arms of the interferometer are appropriately balanced. The absorption of the probe field was detected simultaneously. Without the drive and incoherent pump fields, the absorption and the phase shift show the ordinary features of Doppler-broadened two-level atomic resonance (curve *a* in Fig. 4). When the drive field is present and tuned within the Doppler profile, the absorption spectrum of the probe laser exhibits a narrow transmission peak at the frequency corresponding to that of a two-photon resonance condition. When the incoherent pump is added the narrow gain peak appears (curve *b* in Fig. 4). If the probe field is detuned slightly from the two-photon resonance (point *I* in Fig. 4) the medium is transparent; i.e., it has neither loss nor gain.

The phase shift, which is proportional to the real part of susceptibility, is shown in Figs. 4(ii) and 4(iv). It can be quite large in the transparency region. In particular, we note that at point *I* the change in the refractive index exceeds that found in the same system without the driving field. That is, the real part of the susceptibility is enhanced at the point where the absorption vanishes. We note the good agreement between the theoretical predictions of Fig. 2 and the experimental observations of Fig. 4.

Having observed and analyzed the absorption and dispersion in an optically thin medium we were also able to demonstrate the enhancement of refractive index in an optically dense medium. To accomplish this phase shift and absorption measurements were carried out for

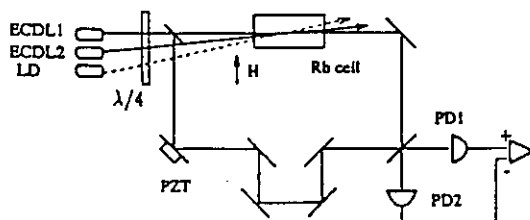


FIG. 3. Schematic of experimental setup. ECDL1 and ECDL2 are probe and driving lasers, respectively; LD is an incoherent pump laser.

a variety of temperatures. Figure 5 shows the value of the phase shift as a function of atomic density. For low temperatures the phase shift in the coherently prepared transparent Rb vapor is somewhat larger than the maximum phase shift in the usual Rb resonant vapor. For temperatures  $T > 80^\circ\text{C}$  ( $N > 3 \times 10^{11} \text{ cm}^{-3}$ ) the Rb absorbs 100% of the probe light near the resonance, i.e., in the region where the refractive index has its maximum. When the drive and incoherent pump are present the system is transparent and displays large phase shifts. The inset in Fig. 5 shows the transmission of the probe laser (curve *A*) and corresponding output  $S_{\text{sig}}$  of the phase shift measurement (curve *B*) at a Rb cell temperature  $\sim 87^\circ\text{C}$ . In the presence of coherent drive and incoherent pumping, the narrow transparency peak appears (curve *a*) on an otherwise flat, completely absorbing background. The corresponding phase shift (curve *b*) measurements display the oscillations which correspond to large values of phase shift. Under the present experimental conditions we observed the phase shifts up to  $\approx 7\pi$  at the point of complete transparency, which corresponds to the resonant change in the refractive index  $\Delta n \sim 10^{-4}$ . We note that such a phase shift is not observable in a usual absorber in the immediate vicinity of resonance because of the resonant absorption.

We remark here that quite large phase shifts accompanied by relatively good transparency can be obtained in a usual nondriven atomic system (e.g., within the Rb  $D_1$  line without coherent preparation) at large detunings. This happens because the real part of the susceptibility  $\chi'$  decreases slower than  $\chi''$  with detuning. However, for large detunings,  $\chi'$  of a usual absorber increases with density much slower than the resonant  $\chi'$ . In particular, for  $N \sim 10^{12} \text{ cm}^{-3}$  we observed that the absorption of the

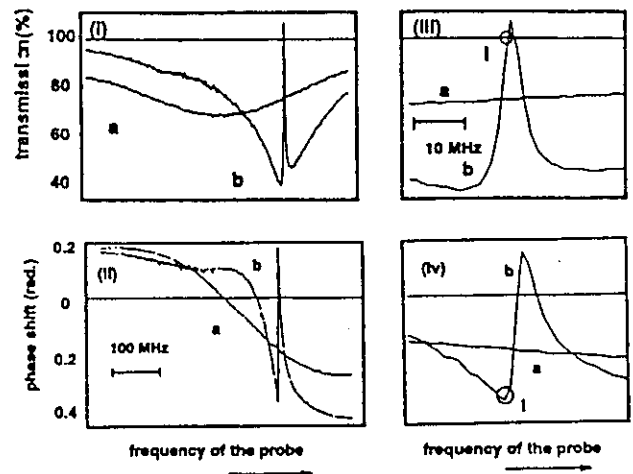


FIG. 4. Transmitted intensity (i,iii) of the probe light in the Rb cell and the difference current of photodetectors, converted into the phase shift (ii,iv). In all figures curve (*a*) was observed without driving and pumping fields, curve (*b*) was observed when those two fields were present.

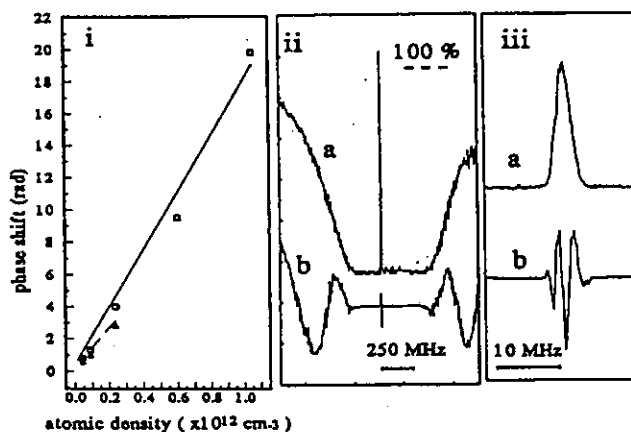


FIG. 5. (i) The phase shifts in Rb vapor as a function of a vapor density.  $\square$  is the phase shift in coherently prepared Rb at the point of complete transparency;  $\Delta$  is the maximum value of phase shift in the same system without coherent preparation. (ii) Transmission of the probe (curve *a*) and corresponding quadrature component of interferometer signal (curve *b*) in an optically dense Rb vapor with driving and incoherent pumping fields present. (iii) The enlarged central part of (ii).

probe field in the nondriven Rb vapor is essentially zero at detuning  $\sim 15$  GHz. In this region the measured phase shift was approximately 1.5 rad.

In conclusion, we have presented an experimental demonstration of an enhancement of the refractive index in a coherently prepared atomic medium accompanied by vanishing absorption. The experimental results were predicted by and are in good agreement with a detailed theoretical analysis.

The authors gratefully acknowledge discussions with E. Arimondo, H. Briegel, M. Fleischhauer, E. Fry, and T. Hänsch, valuable assistance of T. Zibrova, and the support from the Office of Naval Research, the Welch Foundation, the Texas Advanced Research and Technology Program, and the Air Force Office of Scientific Research.

- [1] M.O. Scully, Phys. Rev. Lett. 67, 1855 (1991); M.O. Scully and S.-Y. Zhu, Opt. Commun. 87, 134 (1992); M. Fleischhauer *et al.*, *ibid.* 87, 109 (1992); A.D. Wilson-Gordon and H. Friedman, *ibid.* 94, 238 (1992);

- M. Fleischhauer *et al.*, Phys. Rev. A 46, 1468 (1992); U. Rathe *et al.*, *ibid.* 47, 4994 (1993); J. Dowling and C. Bowden, Phys. Rev. Lett. 70, 1421 (1993); A. Manka *et al.*, *ibid.* 73, 1789 (1994); O. Kocharovskaya, P. Mandel, and M.O. Scully, *ibid.* 74, 2451 (1995).  
 [2] S.E. Harris, J.E. Field, and A. Imamoglu, Phys. Rev. Lett. 64, 1107 (1990).  
 [3] O. Kocharovskaya and Y. Khanin, JETP Lett. 48, 630 (1988); S.E. Harris, Phys. Rev. Lett. 62, 1033 (1989); M.O. Scully, S.-Y. Zhu, and A. Gavrielides, *ibid.* 62, 2813 (1989).  
 [4] K.-J. Boller, A. Imamoglu, and S.E. Harris, Phys. Rev. Lett. 66, 2593 (1991).  
 [5] A. Nottelmann, C. Peters, and W. Lange, Phys. Rev. Lett. 70, 1783 (1993); E.S. Fry *et al.*, *ibid.* 70, 3235 (1993); W.E. van der Veer *et al.*, *ibid.* 70, 3243 (1993).  
 [6] A.S. Zibrov *et al.*, Phys. Rev. Lett. 75, 1499 (1995).  
 [7] G.G. Padmabandu *et al.*, Phys. Rev. Lett. 76, 2053 (1996).  
 [8] S.E. Harris, J.E. Field, and A. Kasapi, Phys. Rev. A 46, R29 (1992).  
 [9] S.E. Harris, Opt. Lett. 19, 2018 (1994).  
 [10] M.O. Scully and M. Fleischhauer, Phys. Rev. Lett. 69, 1360 (1992).  
 [11] M. Xiao *et al.*, Phys. Rev. Lett. 74, 666 (1995); R. Moseley *et al.*, *ibid.* 74, 670 (1995); D. Meschede *et al.*, in Proceedings of CLEO/QELS '95 Boston 1995.  
 [12] G. Alzetta, A. Gozzini, L. Moi, and G. Orriols, Nuovo Cimento Soc. Ital. Fis. 36B, 5 (1976); E. Arimondo and G. Orriols, Nuovo Cimento Lett. 17, 333 (1976); H.R. Gray, R.M. Whitley, and C.R. Stroud, Jr., Opt. Lett. 3, 218 (1978).  
 [13] We note here that the results for  $\chi'$  and  $\chi''$  depend upon the particular choice of the model, e.g., upon the particular incoherent pump mechanism. In the present three-level model, which we use to illustrate the physics, we assume an indirect pump mechanism which populates level *c* via a "one way" pumping from level *b*.  
 [14] A. Imamoglu, J.E. Field, and S.E. Harris, Phys. Rev. Lett. 66, 1154 (1991).  
 [15] In such a configuration probe and driving fields form three effective  $\Lambda$  systems with the Rb  $D_1$  manifold [Fig. 1(b)]. Note that the situation would be different if we used fields with linear polarizations: In that case fields form only two effective  $\Lambda$  systems (since the transition  $2, m_F = 0 \rightarrow 2', m_F = 0$  is forbidden) which implies a large absorption of the probe field on the transition  $1, m_F = 0 \rightarrow 2', m_F = 0$ .